Alfvén solitons in a Fermionic quantum plasma

A. J. Keane,[1] A. Mushtaq,[1,2,*] and M. S. Wheatland[1]
[1]*Sydney Institute for Astronomy, School of Physics, The University of Sydney, New South Wales 2006, Australia*
[2]*TPPD, PINSTECH, P.O. Nilore, Islamabad 44000, Pakistan*
(Received 28 February 2011; published 20 June 2011)

The propagation of Alfvén envelope solitons through a Fermionic quantum plasma is considered. Starting from the governing equations for Hall magnetohydrodynamics including quantum corrections, coupled Zakharov-type equations are derived for circularly polarized Alfvén waves. The equations are numerically solved for time-independent and time-dependent cases. The time-independent case shows that variations in density take the form of dressed density solitons in which an approximately Gaussian peak is surrounded by smaller sinusoidal variations in the density envelope. The mathematical basis for this behavior is explained. A limited time-dependent case is obtained which uses the numerical time-independent soliton solutions as the initial conditions. This confirms that the soliton solutions retain the same profile as they propagate. The relevance of this work to dense astrophysical plasmas like the interiors of white dwarf stars is discussed.

DOI: 10.1103/PhysRevE.83.066407 PACS number(s): 52.27.Gr, 52.35.Bj, 52.35.Mw, 52.65.Kj

I. INTRODUCTION

Alfvén waves play important roles in the heating of and transport of energy in magnetoplasmas and have been studied in a range of contexts, including the solar wind, Earth's magnetosphere, interstellar molecular clouds, and coronal heating [1]. They were first derived from the ideal magnetohydrodynamic (MHD) model, which treats the plasma as a single fluid and provides a macroscopic description of collective effects [2]. If the plasma is assumed to consist of an electron fluid and an ion fluid, dispersion occurs through the appearance of the Hall term.

Equations for the evolution of nonlinear Alfvén wave packets in a cold plasma have been derived from Hall-MHD using a double perturbation technique [3,4]. Considering a weakly nonlinear and weakly dispersive medium gives the derivative nonlinear Schrödinger (DNLS) equation describing the evolution of the magnetic field envelope [5]. In the Hall-MHD model, the wave frequency is comparable to the ion cyclotron frequency and Alfvén waves may couple to plasma oscillations via the ponderomotive force contained in the DNLS equation. A balance between nonlinearity and dispersion gives solutions for small-amplitude Alfvén solitons. A single perturbation approach was applied by Ovenden *et al.* to derive solutions from Hall-MHD for Alfvén solitons of arbitrary amplitude [6].

There has been recent increasing interest in quantum plasmas due to their application to semiconductors, metallic nanodevices and dense astrophysical plasmas [7]. Theory has focused on quantum counterparts to classical plasma models and equations starting from the Schrödinger description of the electron. An ideal MHD model including quantum diffraction and statistical effects has been devised of relevance to the interiors of white dwarfs [8]. A new dispersive Alfvénic wave has also been found, with the dispersion resulting from quantum corrections [9]. Recently, the ideal MHD model has been extended to include spin magnetization, which is important in highly magnetized quantum plasmas such as the atmospheres of neutron stars [10,11]. A new plane-polarized bare Alfvénic soliton arises for pair plasmas produced by a balance between nonlinearity and quantum spin [12].

Including the Hall term allows for investigation of other nonlinear MHD waves in spin-$\frac{1}{2}$ quantum plasmas. Two-dimensional magnetosonic solitons have been studied in two- and three-component plasmas [13,14]. Bare magnetosonic solitons have been found in both one-dimensional [15] and two-dimensional [16] quantum plasmas, with the electron spin-$\frac{1}{2}$ effects modifying the shape of the soliton. Alfvénic wave envelopes have also been investigated in high-β quantum plasmas by using a double perturbation technique which showed that the nonlinear evolution of such waves is described by the DNLS equation [17].

In this article, we demonstrate the existence of Alfvén solitons in a Fermionic quantum plasma with coupling due to the Bohm potential. The organization of the paper is as follows. In Sec. II we present the governing equations for quantum Hall-MHD (QMHD). In Sec. III we derive a set of nonlinear evolution equations from the governing equations using a single perturbation approach like that of Ovenden *et al.* [6]. In Sec. IV nonlinear evolution equations are converted to the stationary frame and numerical solutions are obtained for varying values of the quantum diffraction parameter H_e, the quantum statistical parameter β, and the Alfvén Mach number M_A. In Sec. V, we approximate the velocity of the soliton by its value at the center to obtain a limited nonstationary case which is solved numerically to confirm soliton behavior. Finally, in Sec. VI we summarize our results and discuss their physical significance.

II. GOVERNING EQUATIONS

Consider an electron-ion quantum plasma with background magnetic field in the z direction, $\mathbf{B}_0 = B_0\hat{\mathbf{z}}$. We assume that $\mu_B B_0 \ll k_B T_e$, where k_B is the Boltzmann constant, T_e is the thermodynamic temperature, and $\mu_B = e\hbar/2m_e c$ is the magnitude of the electron magnetic moment (the Bohr magneton). The effects of microscopic spin are negligible. The QMHD model may then be developed starting with the

*Corresponding author: msherpao@gmail.com

momentum equations for electrons and ions in a quantum magnetoplasma [8].

Because Alfvén waves are slowly varying we neglect electron inertia in the electron equation of motion [13]:

$$0 = -\frac{\nabla P_{Fe}}{n_e} - e(\mathbf{E} + \mathbf{u}_e \times \mathbf{B}) + \frac{\hbar^2}{2m_e^2}\nabla\left(\frac{\nabla^2\sqrt{n_e}}{\sqrt{n_e}}\right). \quad (1)$$

Here n_e is the electron fluid density, $\mathbf{u}_e$ is the electron fluid velocity, m_e is the electron mass, $\mathbf{E}$ is the electric field vector, and $\mathbf{B}$ is the magnetic field vector. The third term in (1) represents the quantum diffraction due to quantum tunneling, and $P_{Fe} = [(3\pi^2 m_e)^{2/3}\hbar\, n_e^{5/3}]/5$ is the Fermi pressure for degenerate electrons. In the ion equation of motion,

$$m_i \frac{d\mathbf{u}_i}{dt} = e(\mathbf{E} + \mathbf{u}_i \times \mathbf{B}), \quad (2)$$

we ignore the ion quantum effects due to the large ion inertia. Here n_i is the ion fluid density, $\mathbf{u}_i$ is the ion fluid velocity, m_i is the ion mass, and $d/dt = \partial/\partial t + (\mathbf{u}_i \cdot \nabla)$ is the convective derivative. The ion continuity equation is

$$\frac{\partial n_i}{\partial t} + \nabla \cdot (n_i \mathbf{u}_i) = 0. \quad (3)$$

The two relevant Maxwell's equations are Faraday's law,

$$\nabla \times \mathbf{E} = -\frac{\partial \mathbf{B}}{\partial t}, \quad (4)$$

and Ampère's law,

$$\nabla \times \mathbf{B} = \mu_0 \mathbf{J}, \quad (5)$$

with $\mathbf{J} = e\,(n_i \mathbf{u}_i - n_e \mathbf{u}_e)$. Since we consider low-frequency waves in a highly conductive plasma, the displacement current is neglected. Substituting for $\mathbf{u}_e$ in Eq. (1) from Eq. (5) and using the quasineutrality condition $n_i \approx n_e \approx n$ we have

$$\mathbf{E} = -\left(\mathbf{u}_i - \frac{1}{en\mu_0}\nabla \times \mathbf{B}\right) \times \mathbf{B} - \frac{\nabla P_e}{en} + \frac{\hbar^2}{2m_e^2}\nabla\left(\frac{\nabla^2\sqrt{n}}{\sqrt{n}}\right). \quad (6)$$

We introduce the following rescaling:

$$\mathbf{r} \to \frac{\Omega_i \mathbf{r}}{V_A}, \quad t \to \Omega_i t, \quad \mathbf{u}_i \to \frac{\mathbf{u}_i}{V_A}, \quad \mathbf{B} \to \frac{\mathbf{B}}{B_0}, \quad n \to \frac{n}{n_0}.$$

The subscript zero represents the background quantities, $V_A = B_0/(\mu_0 n_i m_i)^{1/2}$ is the Alfvén speed, and $\Omega_i = (eB_0)/m_i$ is the ion cyclotron frequency. Eliminating $\mathbf{E}$ from Eq. (2) using Eq. (6) gives the normalized effective one-fluid momentum equation:

$$m_i \frac{d\mathbf{u}_i}{dt} = \frac{1}{n}(\nabla \times \mathbf{B}) \times \mathbf{B} - \beta \nabla n^{2/3} + \frac{H_e^2}{2}\nabla\left[\frac{\nabla^2\sqrt{n}}{\sqrt{n}}\right], \quad (7)$$

where $\beta = c_{qs}^2/V_A^2$ measures the quantum statistical effects with $c_{qs} = [(2k_B T_{Fe})/m_i]^{1/2}$ being the quantum ion sound speed and $T_{Fe} = [\hbar^2(3\pi^2 n)^{2/3}]/(2m_e)$ the Fermi temperature. The parameter $H_e = \hbar\,\Omega_i/\sqrt{m_e m_i}V_A^2$ measures the relevance of quantum diffraction effects due to the Bohm potential. Again eliminating $\mathbf{E}$ between Eqs. (2) and (4) gives the normalized magnetic induction equation:

$$\frac{\partial \mathbf{B}}{\partial t} = \nabla \times (\mathbf{u}_i \times \mathbf{B}) - \nabla \times \left[\frac{1}{n}(\nabla \times \mathbf{B}) \times \mathbf{B}\right]. \quad (8)$$

Equations (3), (7), and (8) form the QMHD equations for a magnetized plasma consisting of classical ions and Fermionic electrons.

III. NONLINEAR EVOLUTION EQUATIONS

We consider waves propagating along the z axis. Taking the time derivative of Eq. (8) using Eq. (7) gives

$$\frac{\partial^2 \mathbf{B}}{\partial t^2} = -\frac{d}{dt}\left[\mathbf{B}\frac{\partial u_{iz}}{\partial z} + u_{iz}\frac{\partial \mathbf{B}}{\partial z}\right] + \frac{\partial}{\partial z}\left[\frac{1}{n}(\nabla \times \mathbf{B}) \times \mathbf{B} - \beta \nabla n^{2/3} + \frac{H_e^2}{2}\nabla\left(\frac{\nabla^2\sqrt{n}}{\sqrt{n}}\right)\right] - \nabla \times \frac{d}{dt}\left[\frac{1}{n}(\nabla \times \mathbf{B}) \times \mathbf{B}\right], \quad (9)$$

where u_{iz} is the velocity perturbation in the z direction. Since we are considering circularly polarized Alfvén waves, it is convenient to work with a complex description of the transverse fields. The x and y components of Eq. (9) are combined using $B_\pm = B_x \pm i\,B_y$ to give

$$\frac{\partial^2 B_\pm}{\partial t^2} = \frac{\partial}{\partial z}\left(\frac{1}{n}\frac{\partial B_\pm}{\partial z}\right) + \frac{\partial}{\partial z}\left[u_{iz}\frac{\partial B_\pm}{\partial t} + \frac{d}{dt}(u_{iz}B_\pm)\right] \pm i\,\frac{\partial}{\partial z}\left[\frac{d}{dt}\left(\frac{1}{n}\frac{\partial B_\pm}{\partial z}\right)\right], \quad (10)$$

where B_x and B_y are the wave magnetic field magnitudes in the x and y directions, respectively, and the $\pm$ sign applies for right and left circularly polarized waves, respectively. Taking the time derivative of Eq. (3), using the x and y components of equation (8), and writing in terms of complex fields we have

$$\frac{\partial^2 n}{\partial t^2} - \frac{\beta}{2}\frac{\partial^2 n}{\partial z^2} = u_{iz}\frac{\partial^2}{\partial z^2}(n u_{iz}) + \frac{1}{2}\frac{\partial^2 |B_\pm|^2}{\partial z^2} - H_e^2\frac{\partial}{\partial z}\left[n\frac{\partial}{\partial z}\left(\frac{1}{\sqrt{n}}\frac{\partial^2\sqrt{n}}{\partial z^2}\right)\right]. \quad (11)$$

Equations (3), (10), and (11) are nonlinear equations relating $B_\pm$, n, and u_{iz} in a Fermionic quantum plasma. To determine the changes in $B_\pm$, n, and u_{iz} representing Alfvénic fluctuations the standard perturbation technique of defining a new set of "stretched coordinates" (using $1/\beta$ as a small parameter measuring the importance of dispersive terms) could be applied [17]. However, this technique leaves a higher-order term due to the Bohm potential, which is not included in the resulting nonlinear evolution equations [17]. Instead we linearize Eqs. (3), (10), and (11) by setting $n = 1 + \delta n$ and $u_{iz} = \delta u$, giving

$$\frac{\partial^2 B_\pm}{\partial t^2} - \frac{\partial}{\partial z}\left[(1-\delta n)\frac{\partial B_\pm}{\partial z}\right] + \frac{\partial}{\partial z}\left[\delta u\,\frac{\partial B_\pm}{\partial t} + \frac{d}{dt}(\delta u\, B_\pm)\right] \pm i\frac{\partial^2}{\partial z\,\partial t}\left[(1-\delta n)\frac{\partial B_\pm}{\partial z}\right] = 0, \quad (12)$$

$$\left(\frac{\partial^2}{\partial t^2} - \frac{\beta}{2}\frac{\partial^2}{\partial z^2} + \frac{H_e^2}{2}\frac{\partial^4}{\partial z^4}\right)\delta n = \frac{1}{2}\frac{\partial^2 |B_\pm|^2}{\partial z^2}, \quad (13)$$

and

$$\frac{\partial\,\delta n}{\partial t} + \frac{\partial}{\partial z}(\delta u) = 0. \quad (14)$$

Equation (13) resembles one of the quantum Zakharov equations for Langmuir envelope solitons [18], with the term on the right-hand side being the ponderomotive force. Based on this analogy, we expect modulational instability when variations in n and u_{iz} affect the wave amplitude, which in turn couples to the plasma via the ponderomotive force. This gives an envelope-modulated carrier wave, which may be described using Eqs. (12) and (13) with an ansatz of the form

$$B_{\pm} = b(z,t)\exp\left[i(k_A z - \omega_{\pm} t)\right], \tag{15}$$

such that the carrier waves have frequency $\omega_{\pm}$ and wave number k_A, and the envelope has real amplitude $b(z,t)$. Assuming $\omega_A/\Omega_i \ll 1$ and introducing a stretched time variable τ, where $1/\tau \ll \omega_{\pm} \approx \omega_A$ (see Ref. [6]) gives the set of equations

$$i\left(\frac{\partial}{\partial t} + V_g\frac{\partial}{\partial z}\right)b + \frac{\delta n\,\omega_A}{2}\,b - k_A\,\delta u\,b \mp \frac{1}{2}\frac{\partial^2 b}{\partial z^2} = 0, \tag{16}$$

$$\left(\frac{\partial^2}{\partial t^2} - \beta\frac{\partial^2}{\partial z^2} + \frac{H_e^2}{2}\frac{\partial^4}{\partial z^4}\right)\delta n = \frac{1}{2}\frac{\partial^2 |b|^2}{\partial z^2}, \tag{17}$$

and

$$\frac{\partial\,\delta n}{\partial t} + \frac{\partial}{\partial z}(\delta u) = 0, \tag{18}$$

where $V_g \simeq 1 \mp k_A$ is the normalized group velocity of the original wave, with $k_A \approx \omega_A$ for small amplitudes in the magnetic perturbation. Equations (16)–(18) are the nonlinear evolution equations describing the perturbations in the magnetic field $b(z,t)$, the plasma number density $\delta n(z,t)$, and velocity $\delta u(z,t)$ for a nonlinear wave packet propagating in the z direction through a dispersive quantum plasma. For the case $H_e = 0$ and $\beta = c_s^2/V_A^2$ with $c_s = [(k_B T_e)/m_i]^{1/2}$ representing the ion sound speed, Eqs. (16)–(18) reduce to the nonlinear evolution equations for a classical plasma derived by Ovenden *et al.* [6].

IV. TIME-INDEPENDENT ALFVÉN SOLITONS

A. Mathematical formulation

We seek a stationary version of the coupled Eqs. (16)–(18). Accordingly, we apply the Galilean transformation,

$$\varepsilon = z - M_A t, \tag{19}$$

replacing the dependent variables according to

$$\begin{aligned} b(z,t) &\to b(\varepsilon)\exp\left[i\zeta t\right],\\ \delta n(z,t) &\to \delta n(\varepsilon), \quad \text{and}\\ \delta u(z,t) &\to \delta u(\varepsilon). \end{aligned} \tag{20}$$

The new independent variable ε is the spatial coordinate of the frame of reference moving with the soliton at the Alfvén Mach number,

$$M_A = \frac{u_0}{V_A}, \tag{21}$$

where u_0 is the velocity of the wave packet. With these transformations, Eqs. (16)–(18) reduce to the coupled nonlinear ordinary differential equations

$$(1 - M_A)(1 - 2M_A)\,\delta n\,b - \zeta b + \frac{d^2 b}{d\varepsilon^2} = 0 \tag{22}$$

and

$$H_e^2\frac{d^2\delta n}{d\varepsilon^2} + 2\left(M_A^2 - \beta\right)\delta n - |b|^2 = 0, \tag{23}$$

with $V_g = M_A$ and $k_A = 1 - M_A$. The parameter ζ is an arbitrary constant which scales the amplitude of the soliton solution for the stationary case, and is set to $\zeta = 1$ for all calculations except where otherwise noted. equations (22) and (23) are for the left-hand polarized wave (corresponding to ω_+) since in the classical case the right-hand wave (ω_-) is always modulationally stable [4]. We aim to find soliton solutions for the envelope magnetic field $b(\varepsilon)$ and density perturbation $\delta n(\varepsilon)$ for varying values of the quantum diffraction parameter H_e, the quantum statistical parameter β, and the Alfvén Mach number M_A. Envelope solitons are localized [19], so appropriate boundary conditions are

$$b(\varepsilon) \to 0 \quad \text{and} \quad \delta n(\varepsilon) \to 0 \quad \text{as} \quad \varepsilon \to \pm\infty. \tag{24}$$

B. Numerical solutions

Equations (22) and (23) are solved numerically using two methods in which the boundary conditions (24) are applied at finite but large values of ε ($\varepsilon = \pm 10$). The relaxation method replaces the second derivatives with centered difference approximations and solves the resulting nonlinear system of equations using Newton's method [20]. The shooting method treats Eqs. (22) and (23) as an initial value problem by fixing one boundary value and guessing another. The equations are integrated using an adaptive fifth-order Runge-Kutta scheme [21], updating the guessed initial value via Newton's method until the boundary conditions are met [20]. The results presented in this section are those found using the relaxation method with 1000 equidistant grid points.

In the classical case ($H_e = 0$ and $\beta = c_s^2/V_A^2$) Eqs. (22) and (23) admit the analytic solutions

$$b(\varepsilon) = \sqrt{\frac{2\zeta\left(M_A^2 - \beta\right)}{(1 - M_A)(1 - 2M_A)}}\,\mathrm{sech}\left(\sqrt{\zeta}\,\varepsilon\right) \tag{25}$$

and

$$\delta n(\varepsilon) = \frac{[b(\varepsilon)]^2}{2\left(M_A^2 - \beta\right)}. \tag{26}$$

Equations (25) and (26) are used as an initial guess for both numerical schemes and to compare results for solitons in a quantum plasma with the classical solution.

Figure 1 shows the numerically calculated soliton solutions for an Alfvén Mach number $M_A = 1.4$ in a quantum plasma with $\beta = 1$. The solid line shows the case $H_e = 0.12$ and the dashed line shows the case $H_e = 0.24$. The solution with $H_e = 0.12$ differs only slightly from the classical case, retaining an approximate Gaussian profile for $b(\varepsilon)$ and $\delta n(\varepsilon)$. For $H_e = 0.24$ the perturbation in $b(\varepsilon)$ has a similar but slightly narrower profile. However, the density perturbation $\delta n(\varepsilon)$ has a new feature: Small sinusoidal variations in density occur on either side of the main density peak, forming a "dressed soliton" [22]. The main density peak of the solution for $H_e = 0.24$ is also narrower and of greater amplitude than for $H_e = 0.12$ while the dressed density oscillations have a constant amplitude and wavelength. Additional calculations show that the wavelength

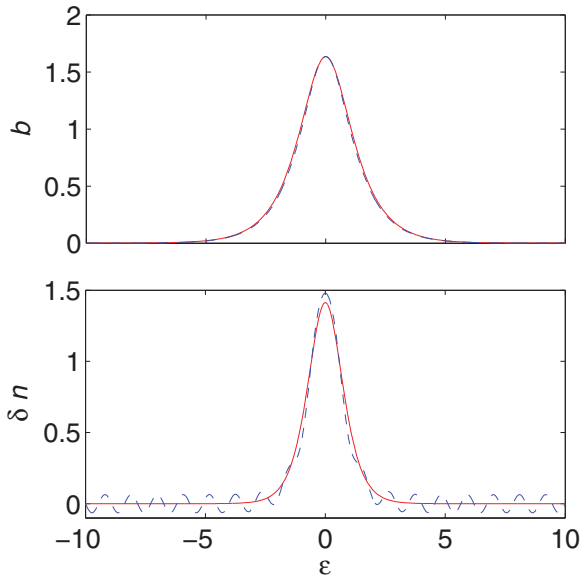

FIG. 1. (Color online) Stationary solutions using the relaxation method for a super-Alfvénic soliton ($M_A = 1.4$) in a quantum plasma with $\beta = 1$. The solid line is the solution obtained for $H_e = 0.12$ and the dashed line is the solution obtained for $H_e = 0.24$.

and amplitude of these oscillations increases with H_e, but the amplitude does not increase monotonically as a function of H_e.

Figure 2 shows numerical super-Alfvénic soliton solutions ($M_A > 1$) for a quantum plasma with $\beta = 1$ and $H_e = 0.12$. The solid line shows the case $M_A = 1.1$ and the dashed line shows the case $M_A = 1.7$. For $M_A = 1.1$, the perturbation in both $b(\varepsilon)$ and $\delta n(\varepsilon)$ is wider and of greater amplitude compared with the case $M_A = 1.4$ (Fig. 1), and the density perturbation is a dressed soliton. For the larger value of $M_A = 1.7$, the perturbations in both $b(\varepsilon)$ and $\delta n(\varepsilon)$ are narrower and of

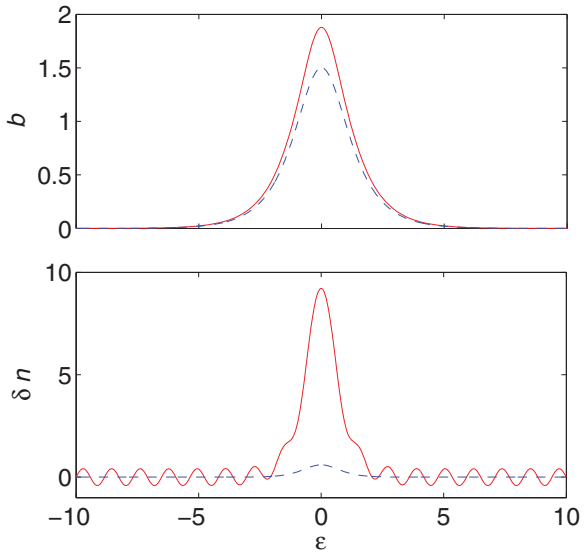

FIG. 2. (Color online) Stationary solutions using the relaxation method for super-Alfvénic solitons ($M_A > 1$) in a quantum plasma with $\beta = 1$ and $H_e = 0.12$. The solid line is the solution obtained for $M_A = 1.1$ and the dashed line is the solution obtained for $M_A = 1.7$.

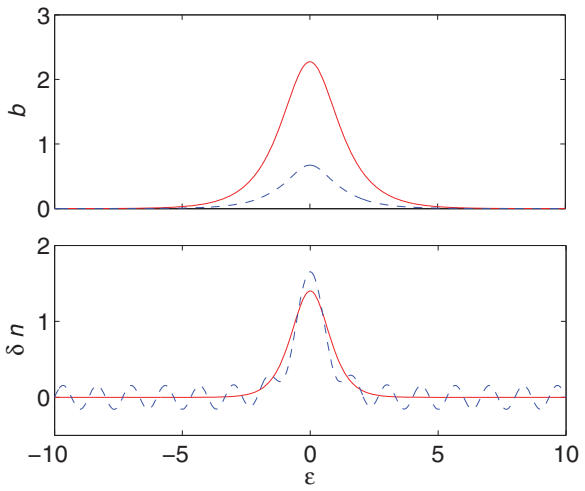

FIG. 3. (Color online) Stationary solutions using the relaxation method for a super-Alfvénic soliton ($M_A = 1.4$) in a quantum plasma with $H_e = 0.12$. The solid line is the solution obtained for $\beta = 0.1$ and the solid line is the solution obtained for $\beta = 1.8$.

smaller amplitude than the case $M_A = 1.4$. Based on additional calculations, we find that, in common with the classical case given by Eqs. (25) and (26), the amplitudes of $b(\varepsilon)$ and $\delta n(\varepsilon)$ become arbitrarily large as $M_A \to 1$. However, the dressed density oscillations also increase in amplitude, such that as $M_A \to 1$, they begin to dominate over the central peak in density.

Figure 3 shows the numerical solutions for a soliton with Alfvén Mach number $M_A = 1.4$ in a quantum plasma with $H_e = 0.12$ for two values of β: The solid line shows the case $\beta = 0.1$ and the dashed line shows the case $\beta = 1.8$. The solution for $\beta = 0.1$ has a similar profile for $\delta n(\varepsilon)$ to the case $\beta = 1$ (Fig. 1) but $b(\varepsilon)$ is of larger amplitude and width. Conversely, the solution for $\beta = 1.8$ has a $b(\varepsilon)$ peak of smaller amplitude and width by comparison with the case $\beta = 1$. In this case a dressed density soliton occurs with a non-Gaussian peak and the dressed oscillations have greater amplitude than the case $\beta = 1$. Additional calculations confirm that as $\beta \to M_A^2$, the amplitude and wavelength of the dressed density oscillations increase until they dominate over the central peak, although the amplitude does not increase monotonically as a function of β. However, dressed soliton solutions are only found when $H_e > 0$. For $\beta \geqslant M_A^2$ no soliton solutions are found [this applies also for the classical case since Eq. (25) has a negative root when $\beta \geqslant M_A^2$ and $M_A > 1$].

Figure 4 shows the numerical sub-Alfvénic soliton solutions ($M_A = 0.65$) for a quantum plasma with $\beta = 1$. The solid line shows the case $H_e = 0$ and the dashed line shows the case $H_e = 2.0$. With $H_e = 0$, there is a bright soliton for $b(\varepsilon)$, but a dark soliton for $\delta n(\varepsilon)$, that is, a central rarefaction in the background density. With $H_e = 2.0$, the solution for $\delta n(\varepsilon)$ is of greater amplitude and width compared with $H_e = 0$. The density perturbation $\delta n(\varepsilon)$ is again a dark soliton, but is wider and of smaller amplitude compared with $H_e = 0$. Dressed density oscillations do not appear. Further calculations show that dark soliton solutions only occur if $M_A^2 \leqslant \beta$ and $0.5 < M_A < 1$, which is also the case for classical plasmas as seen with Eqs. (25) and (26). Note that the scaling parameter

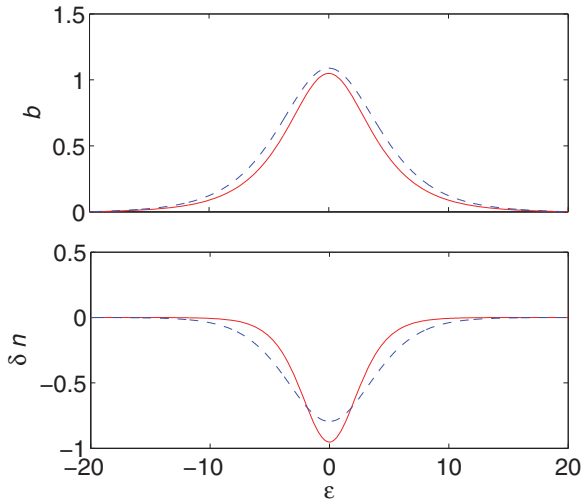

FIG. 4. (Color online) Stationary solutions using the relaxation method for a sub-Alfvénic soliton ($M_A = 0.65$) in a quantum plasma with $\beta = 1$. The solid line is the solution obtained for $H_e = 0$ and the dashed line is the solution obtained for $H_e = 2$.

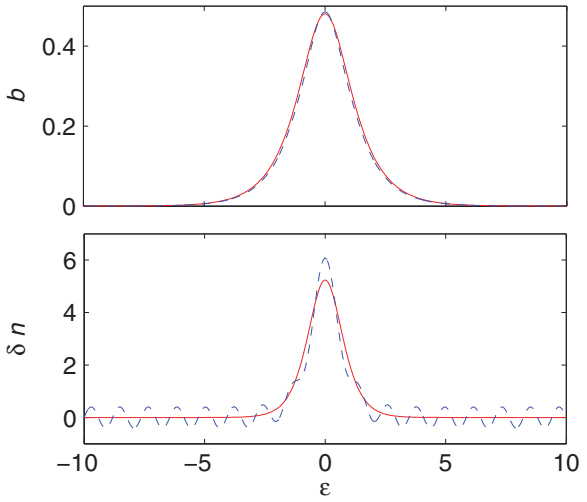

FIG. 5. (Color online) Stationary solutions using the relaxation method for a sub-Alfvénic soliton ($M_A = 0.35$) in a quantum plasma with $\beta = 0.1$. The solid line is the solution obtained for $H_e = 0.02$ and the dashed line is the solution obtained for $H_e = 0.04$.

used for Fig. 4 is chosen to be $\zeta = 0.1$ to obtain dark soliton solutions with $\delta n(\varepsilon) > -1$. Below this value the solutions are unphysical since they correspond to a negative plasma density.

Figure 5 shows numerical sub-Alfvénic soliton solutions ($M_A = 0.35$) in a quantum plasma with a smaller statistical parameter $\beta = 0.1$. The solid line shows the case $H_e = 0.02$ and the dashed line shows the case $H_e = 0.04$. For $H_e = 0.02$, the solution retains an approximately Gaussian profile in both $b(\varepsilon)$ and $\delta n(\varepsilon)$ similar to the classical case given by Eqs. (25) and (26). For $H_e = 0.04$, the solution for $b(\varepsilon)$ retains a classical profile, but a dressed soliton occurs for $\delta n(\varepsilon)$. The peak of $\delta n(\varepsilon)$ is non-Gaussian and exhibits side lobes and is of greater amplitude than for $H_e = 0.02$. Further investigations show that for $M_A^2 > \beta$ the dressed density oscillations dominate as $M_A \to \beta$. For $M_A^2 < \beta$, dressed density oscillations do not occur and the solution resembles the classical case, with the amplitudes of $b(\varepsilon)$ and $\delta n(\varepsilon)$ approaching zero as $M_A \to 0$.

The relaxation method results may be checked by comparison with the shooting method. It is found that for envelope soliton solutions, the average discrepancy in $b(\varepsilon)$ and $\delta n(\varepsilon)$ between the two methods is $\sim 10^{-6}$ to $\sim 10^{-5}$. The dressed soliton solutions in Figs. 1–5 are reproduced with the shooting method and the average discrepancy in $\delta n(\varepsilon)$ is $\sim 10^{-4}$ to $\sim 10^{-3}$. The stated discrepancies indicate close agreement between results obtained with the two methods and confirm the accuracy of the numerical solutions.

C. Analytical insight

The observed behavior may be understood analytically. Assuming $b(\varepsilon) = 0$, equations (22) and (23) reduce to

$$H_e^2 \frac{d^2 \delta n}{d\varepsilon^2} = -2\left(M_A^2 - \beta\right) \delta n. \tag{27}$$

When $M_A^2 > \beta$, Eq. (27) has the analytical solution

$$\delta n(\varepsilon) = A \cos\left(\frac{2\pi\varepsilon}{\lambda}\right), \tag{28}$$

where

$$\lambda = \sqrt{\frac{2\pi^2 H_e^2}{M_A^2 - \beta}} \tag{29}$$

and where A is an arbitrary amplitude. Equation (27) applies away from the soliton peak provided $b(\varepsilon) = 0$. Hence, it describes the equations in the absence of the soliton perturbation. If $H_e = 0$, Eq. (27) becomes $\delta n(\varepsilon) = 0$, indicating that in the absence of quantum diffraction, there are no sinusoidal variations in density. As H_e increases, Eq. (28) superimposes harmonic spatial variation onto the soliton solution for δn. Equation (29) shows that for larger values of H_e the density oscillations have larger wavelengths λ, in agreement with the calculations in the previous section. Equation (29) also shows that as $M_A^2 \to \beta$, the density oscillations have larger wavelengths, again in agreement with calculations.

If $M_A^2 < \beta$ the change of sign on the right-hand side of Eq. (27) results in the analytical solution

$$\delta n(\varepsilon) = A \cosh\left[\frac{\varepsilon}{H_e}\sqrt{2\left(M_A^2 - \beta\right)}\right], \tag{30}$$

where A is an arbitrary amplitude. Hyperbolic functions are not periodic and hence there are no dressed density perturbations in the sub-Alfvénic case, which explains why no dressed density solitons are seen in Fig. 4 or for the case $M_A^2 < \beta$ discussed in relation to Fig. 5.

V. TIME-DEPENDENT ALFVÉN SOLITONS

The nonlinear evolution Eqs. (16)–(18) may be solved for nonstationary soliton solutions for a quantum plasma. We consider a limited case. The velocity perturbation δu may be approximated by its value at the center of the envelope

$$\delta u(z,t) = V_g \, \delta n(z,t), \tag{31}$$

which is accurate provided $z \approx M_A t$ [6]. Assuming $V_g = M_A$ gives

$$i\left(\frac{\partial}{\partial t} + M_A \frac{\partial}{\partial z}\right) b + \frac{1}{2}(1 - M_A)(1 - 2M_A)\, b\, \delta n + \frac{1}{2}\frac{\partial^2 b}{\partial z^2} = 0 \tag{32}$$

and

$$\left(\frac{\partial^2}{\partial t^2} - \beta \frac{\partial^2}{\partial z^2} + \frac{H_e^2}{2}\frac{\partial^4}{\partial z^4}\right) \delta n = \frac{1}{2}\frac{\partial\, |b|^2}{\partial z^2}. \tag{33}$$

Equations (32) and (33) represent a limited nonstationary case for testing the results. To implement the numerical method, the periodic boundary conditions

$$b(-z_{\max}) = b(z_{\max}) \quad \text{and} \quad \delta n(-z_{\max}) = \delta n(z_{\max}) \tag{34}$$

are used in a computational domain with $-z_{\max} \leqslant z \leqslant z_{\max}$. The solutions subject to (34) "wrap around" the domain and so can propagate for any length of time. The stationary solutions obtained in Sec. IV B. using the relaxation method are used as initial conditions for the time-dependent calculation. The initial condition is propagated in time by solving Eqs. (32) and (33) numerically.

A naive numerical method uses a forward derivative approximation to the time derivatives of each equation and a centered derivative approximation to the spatial derivatives of each equation [20]. For Eq. (33), the difference scheme is

$$\begin{aligned}\frac{\delta n_j^{k+1} - 2\delta n_j^k + \delta n_j^{k-1}}{(\Delta t)^2} &= \frac{\beta}{(\Delta z)^2}\left(\delta n_{j+1}^k - 2\delta n_j^k + \delta n_{j-1}^k\right) \\ &\quad - \frac{H_e^2}{2(\Delta z)^4}\left(\delta n_{j+2}^k - 4\delta n_{j+1}^k + 6\delta n_j^k - 4\delta n_{j-1}^k + \delta n_{j-2}^k\right) \\ &\quad + \frac{1}{2(\Delta z)^2}\left(\left|b_{j+1}^k\right|^2 - 2\left|b_j^k\right|^2 + \left|b_{j-1}^k\right|^2\right),\end{aligned} \tag{35}$$

where $b_j^k = b(x_j, t^k)$ and $\delta n_j^k = \delta n(x_j, t^k)$, with spatial step j and time step k. However, for Eq. (32) this method is inappropriate, since for complex Schrödinger-like equations the naive method is unconditionally unstable [23]. Hence, we apply a Crank-Nicolson scheme to Eq. (32), in which the spatial derivatives are approximated at the average of two time steps [20]. To simplify calculations, the nonlinear term $\delta n(z,t)$ is linearized by only evaluating it at one time step [24]. For Eq. (32), the difference scheme is

$$\begin{aligned}i\left(\frac{b_j^{k+1} - b_j^k}{\Delta t}\right) &= \frac{i\, M_A}{\Delta z}\left(\frac{1}{2}\left[b_{j+1}^{k+1} - b_{j-1}^{k+1}\right] + \frac{1}{2}\left[b_{j+1}^k - b_{j-1}^k\right]\right) \\ &\quad - \frac{1}{2}(1 - M_A)(1 - 2M_A)\frac{1}{2}\left(b_j^{k+1} + b_j^k\right)\delta n_j^k \\ &\quad - \frac{1}{2(\Delta z)^2}\left(\frac{1}{2}\left[b_{j+1}^{k+1} - 2b_j^{k+1} + b_{j-1}^{k+1}\right]\right. \\ &\quad \left. + \frac{1}{2}\left[b_{j+1}^k - 2b_j^k + b_{j-1}^k\right]\right).\end{aligned} \tag{36}$$

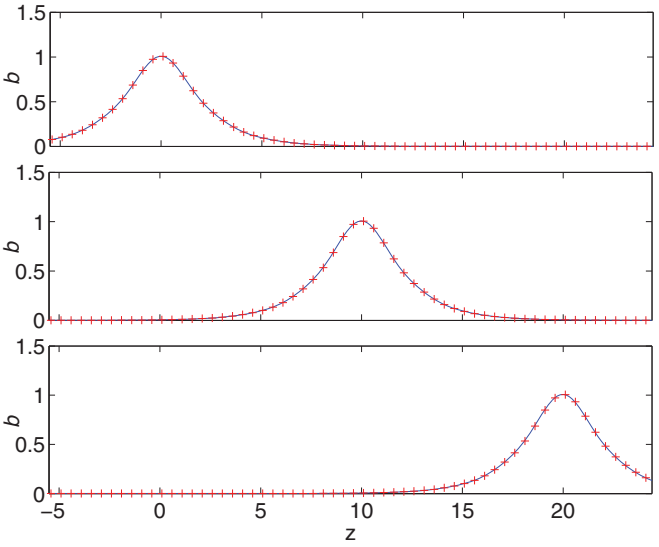

FIG. 6. (Color online) Nonstationary solutions for the magnetic envelope $b(z,t)$ for a super-Alfvénic soliton ($M_A = 1.25$) in a quantum plasma with $\beta = 1$ and $H_e = 0.4$. The solid lines show the numerical solution and the crosses the stationary solution translated in time. The solution is shown at times $t = 0$ (top), $t = 8$ (middle), and $t = 16$ (bottom).

The numerical scheme updates Eqs. (35) and (36) simultaneously.

Figures 6 and 7 show the numerical solutions for $b(z,t)$ and $\delta n(z,t)$, respectively, for a super-Alfvénic soliton ($M_A = 1.25$) in a quantum plasma with $\beta = 1$ and $H_e = 0.4$ at times $t = 0$ (top panel), $t = 8$ (middle panel), and $t = 16$ (bottom panel). The solid lines represent the numerical solutions, and the superimposed crosses are the stationary solutions used as the

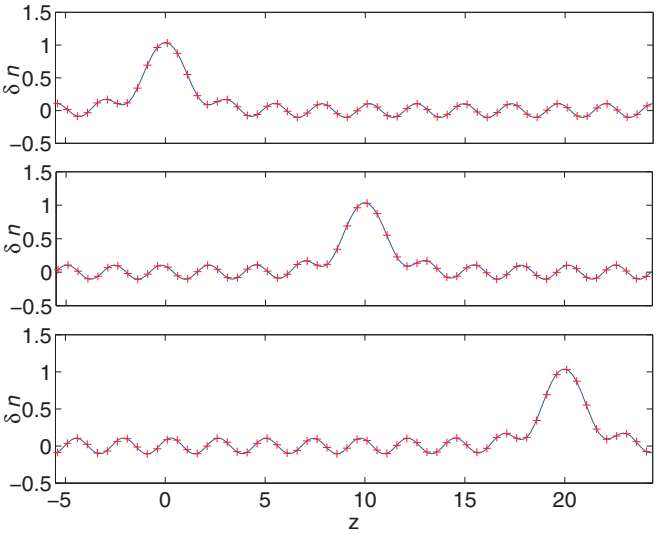

FIG. 7. (Color online) Nonstationary solutions for the dressed density perturbation $\delta n(z,t)$ for a super-Alfvénic soliton ($M_A = 1.25$) in a quantum plasma with $\beta = 1$ and $H_e = 0.4$. The solid lines show the numerical solution and the crosses the stationary solution translated in time. The solution is shown at times $t = 0$ (top), $t = 8$ (middle), and $t = 16$ (bottom).

initial conditions, translated in space by $z = M_A t$. The results show that the shape of the numerical solutions is unchanged during propagation. This is the defining characteristic of a soliton and confirms the stationary solutions computed in Sec. IV.

Due to its explicit formulation, the numerical scheme (35) for the wave equation (33) is only stable for sufficiently small time steps. When $H_e = 0$ the appropriate stability condition is the Courant-Friedrichs-Lewy condition [20]. As H_e is increased, the stability criterion is found to be more stringent than the Courant-Friedrich-Lewy condition, leading to long computation times. This could be avoided by using the method of lines [25], which discretizes spatial derivatives but does not discretize the time derivatives, and then solves the resulting system of equations simultaneously. The advantage of such a scheme is that it is fully implicit and so unconditionally stable. A method which solves the system of equations simultaneously could also be applied to the original nonlinear equations given by (16)–(18). These equations are not solvable using a scheme like that of Eqs. (35) and (36) because the system of equations is coupled via the time derivative of $\delta n(z,t)$.

VI. DISCUSSION AND CONCLUSION

In this paper we use the QMHD model to derive nonlinear evolution equations for Alfvén waves with magnetic field b, density perturbation δn, and velocity δu in a quantum plasma. We find soliton solutions for the stationary case by assuming localized boundary conditions and using two numerical schemes, namely the shooting method and the relaxation method. The solutions obtained with the two schemes agree and confirm the existence of soliton solutions. An interesting feature is the appearance of "dressed density" soliton solutions, that is, solutions with oscillatory density perturbations on either side of the soliton peak. These solutions appear for values $H_e \gtrsim 10^{-2}$ of the quantum diffraction parameter. The size and wavelength of the dressed density solitons is found to increase with H_e, but the solutions are also affected by the value of the quantum statistical parameter β and the Alfvén Mach number M_A. In particular, as $\beta \to M_A^2$ the size and wavelength of the dressed density solitons increases, provided $H_e > 0$. For $0.5 < M_A < 1$ dark density solitons may occur when $\beta > 0.5$ but without density oscillations. By approximating the velocity perturbation δu by its value in the center of the wave envelope, a set of equations is derived for a limited nonstationary case. The stationary solutions obtained with the relaxation method are used as initial conditions for the nonstationary equations, which are solved using a finite difference scheme with periodic boundary conditions. The solutions are found to retain their shape as they propagate, as expected for a soliton.

Dressed envelope soliton solutions have previously been found in classical plasma regimes such as when quasineutrality is not assumed for Langmuir envelope solitons [26]. The dressed density solitons found here may result from the competition between the higher-order dispersive term $(H_e^2/2)\,\partial^4 \delta n/\partial z^4$ in Eq. (13) associated with quantum diffraction, and the nonlinear ponderomotive force. The H_e term has been included in calculations for Langmuir envelope solitons in a quantum plasma where it was found to result in dressed envelope solitons [27]. However, the earlier study showed that when H_e was increased, the oscillatory tails of Langmuir solitons were smoothed out. Section IV shows that the dressed Alfvén solitons have oscillatory tails which increase in amplitude as H_e is increased.

The envelope solitons and dressed envelope solitons found here are distinct solutions and the switch between the two is found to occur over a small increase in the quantum parameter of order $\Delta H_e \sim 10^{-2}$. The dressed density solitons are not localized in the sense that there is a localized envelope-soliton-like profile for the density perturbation but the surrounding sinusoidal variations take nontrivial values of δn and $\partial \delta n/\partial z$ near the boundaries. For small-amplitude oscillations, the solution may be considered "nearly localized" but it should be noted that the boundary conditions given by (24) fix the sinusoidal solutions to $\delta n = 0$ at the boundaries.

Figures 1 and 4 show that for both sub- and super-Alfvénic solitons, the solution for the main density peak increases in amplitude and narrows as H_e is increased, while Fig. 5 shows that the dark density soliton decreases in amplitude and becomes wider. Since H_e represents quantum diffraction, the electrons are able to tunnel into the region of perturbed density associated with the central peak such that the average value of δn is greater over the central peak. The quantum tunneling directly affects the electron density, so this could explain why the solutions for δn are significantly different from the classical case when the Bohm term is included, in contrast to the solutions for b.

The solutions obtained here may apply in certain astrophysical scenarios, specifically dense plasmas in the atmosphere of neutron stars and the interior of massive white dwarfs. In these locations, the plasma parameters may be $n_0 \approx 10^{29} - 10^{34}\ m^{-3}$, $T_{Fe} \approx 10^5 - 10^7\ K$, and $B_0 \approx 10^9 - 10^{14}\ G$. Using SI units, the quantum diffraction parameter is $H_e \sim 10^{-30}\,(n_0/B_0)$ and the quantum statistical parameter is $\beta \sim 10^{-28}\,(T_{Fe}\, n_0/B_0^2)$ [13]. The stated astrophysical parameters give $H_e \lesssim 10^{-1}$ and β also has a finite value, which may be of order unity. The appearance of dressed density solitons coincides with the upper limit of n_0 and the lower limit of B_0. Hence, these solutions may apply in this astrophysical scenario. However, for the range of magnetic field strengths specified above, spin magnetization is likely to be important. Further studies could incorporate the spin force $\mathbf{F}_s = -2n_e \tanh[(\mu_B B)/T_e]\mu_B \nabla \mathbf{B}$ [10] (with T_e being the thermodynamic temperature of an electron) for fluid models to derive evolution equations for nonlinear Alfvén waves of arbitrary amplitude in a spin-$\frac{1}{2}$ quantum plasma.

ACKNOWLEDGMENTS

One of the authors (A. J. Keane) would like to thank Dr. Neil Cramer for useful discussions and acknowledges support from the School of Physics at the University of Sydney. We also greatly appreciate the input of Professor Don Melrose during the drafting process.

[1] N. F. Cramer, *The Physics of Alfvén Waves* (Wiley, Berlin, 2001).
[2] H. Alfvén, Nature (London) **150**, 405 (1942).
[3] E. Mjølhus, J. Plasma Phys. **16**, 321 (1976).
[4] K. Mio, T. Ogmo, K. Minami, and S. Takeda, J. Phys. Soc. Jpn. **41**, 265 (1976).
[5] E. Mjølhus and J. Wyler, Phys. Scr. **33**, 442 (1986).
[6] C. R. Ovenden, H. A. Shah, and S. J. Schwartz, J. Geophys. Res. **88**, 6095 (1983).
[7] G. Manfredi, Fields Inst. Commun. **46**, 263 (2005).
[8] F. Haas, Phys. Plasmas **12**, 062117 (2005).
[9] P. K. Shukla and L. Stenflo, New J. Phys. **8**, 111 (2006).
[10] G. Brodin and M. Marklund, New J. Phys. **9**, 277 (2007).
[11] M. Marklund and G. Brodin, Phys. Rev. Lett. **98**, 025001 (2007).
[12] G. Brodin and M. Marklund, Phys. Plasmas **14**, 112107 (2007).
[13] A. Mushtaq and A. Qamar, Phys. Plasmas **16**, 022301 (2009).
[14] W. Masood, H. A. Shah, A. Mushtaq, and M. Salimullah, J. Plasma Phys. **75**, 217 (2009).
[15] M. Marklund, B. Eliasson, and P. K. Shukla, Phys. Rev. E **76**, 067401 (2007).
[16] A. Mushtaq and S. V. Vladimirov, Phys. Plasmas **17**, 102310 (2010).
[17] A. P. Misra, N. K. Ghosh, and P. K. Shukla, Phys. Plasmas **16**, 102309 (2009).
[18] L. G. Garcia, F. Haas, L. P. L. Oliveira, and J. Goedert, Phys. Plasmas **12**, 012302 (2005).
[19] P. G. Drazin and R. S. Johnson, *Solitons: An Introduction* (Cambridge University Press, Cambridge, 1989).
[20] W. H. Press, S. A. Teukolsky, W. T. Vetterling, and B. P. Flannery, *Numerical Recipes: The Art of Scientific Computing* (Cambridge University Press, Cambridge, 2007).
[21] J. R. Dormand and P. J. Prince, J. Comput. Phys. Appl. Math. **6**, (1980).
[22] K. Konno, T. Mitsuhashi, and Y. H. Ichikawa, J. Phys. Soc. Jpn. **43**, 669 (1977).
[23] T. F. Chan, SIAM J. Numer. Anal. **23**, 274 (1986)
[24] P. Li, Comput. Phys. Commun. **88**, 121 (1995).
[25] W. E. Schiesser and G. W. Griffiths, *A Compendium of Partial Differential Equation Models: Method of Lines Analysis with Matlab* (Cambridge University Press, Cambridge, 2009).
[26] P. Deeskow, H. Schamel, N. N. Rao, M. Y. Yu, R. K. Varma, and P. K. Shukla, Phys. Fluids **30**, 2703 (1987).
[27] P. K. Shukla and B. Eliasson, Phys. Lett. A **372**, 2893 (2008).